SYNTHESIS OF TiO_2 NANOPARTICLES USING DURIAN PEEL EXTRACT FOR INDIGO CARMINE DYES PHOTOCATALYTIC DEGRADATION

Dosi Novita Sari[1], Khoiriah Khoiriah[2], Romy Dwipa Yamesa Away[1], Asmida Herawati[3], Reza Audina Putri[2], Vivi Sisca[4], Tia Okselni[5]

[1]*Department of Chemistry, Faculty of Mathematics and Natural Sciences Padang State University, Padang 25173 Indonesia, dosinovitasari656@gmail.com (D.N.S.); romydwipa@fmipa.unp.ac.id (R.D.Y.).*
[2]*Research Center for Catalysis, National Research and Innovation Agency Serpong, Banten 15314, Indonesia, khoi013@brin.go.id (K.K.); reza012@brin.go.id (R.A.P.).*
[3]*Research Center for Photonics, National Research and Innovation Agency Serpong, Banten 15314, Indonesia, asmi002@brin.go.id (A.H.).*
[4]*Research Center for Molecular Chemistry, National Research and Innovation Agency Serpong, Banten, 1531, Indonesia, vivi009@brin.go.id (V.S.).*
[5]*Research Center for Pharmaceutical Ingedients and Traditional Medicine National Research and Innovation Agency, Cibinong West Java 16911, Indonesia, okselni@gmail.com (O.T.).*

Received 12 January 2026
Accepted 04 April 2026
DOI: 10.59957/jctm.v61.i4.2026.8

ABSTRACT

TiO_2 nanoparticles were successfully synthesized via a sol - gel using Durian (Durio zibethinus) peel extract as a green and sustainable approach for photocatalytic applications. The peel extract acted as a natural stabilizing and capping agent, with its bioactive compounds promoting the formation of nanocrystalline anatase (5 - 10 nm) exhibiting good colloidal stability and a bandgap of 3.2 eV. Photocatalytic evaluation showed that the bio-based TiO_2 nearly achieved ± 99 % degradation of indigo carmine within 60 min, comparable to commercial TiO_2. According to the result, utilization of durian peel extract for TiO_2 synthesis offers a sustainable strategy with potential application in textile wastewater treatment and contributing to circular economy practices.

Keywords: durian peel, green synthesis, indigo carmine, TiO_2 photocatalyst.

INTRODUCTION

Synthetic dyes are among the most persistent sources of aquatic pollution worldwide because of their extensive use in the textile, paper, and plastic industries. An estimated 15 % of global dye production is discharged into the environment, significantly increasing the chemical oxygen demand (COD) and threatening aquatic ecosystems [1]. Among these dyes, indigo carmine ($C_{16}H_8N_2Na_2O_8S_2$) is widely used because of its intense blue colour, high solubility, and strong stability provided by azo bonds (-C=C-). However, these properties also render indigo carmine highly resistant to natural degradation and toxic to aquatic organisms [2, 3].

Conventional wastewater treatment methods, including coagulation, electro - decolorization, and biological processes, have been used to remove dyes. However, these approaches suffer from significant drawbacks, such as high operational costs, complex procedures, and the risk of secondary.

Pollutants are more hazardous than their parent compounds [4 - 6]. Advanced oxidation processes (AOPs) have emerged as promising alternatives to overcome these limitations.

Among AOPs, photocatalysis using titanium dioxide (TiO_2), has attracted particular attention. Under ultraviolet irradiation, TiO_2 generates reactive oxygen species (•OH, $•O_2^-$) that can mineralize organic pollutants into harmless end products, such as CO_2 and H_2O [7]. TiO_2 is favoured for its high stability, nontoxicity,

and cost-effectiveness. However, conventional TiO_2 synthesis routes often rely on hazardous chemicals, raising environmental and safety concerns [8].

Green synthesis methods employing plant extracts have been recently explored as sustainable alternatives to conventional methods. Biomolecules, such as flavonoids, tannins, phenolics, and terpenoid, can act as natural reducing and stabilizing agents during nanoparticle formation [9]. Durian peel (*Durio zibethinus*), an abundant agicultural by-product in Indonesia, contains high levels of cellulose 50 - 60 %, is also rich in secondary metabolites including flavonoid, tannins, saponins, alkaloids, phenolics, and terpenoids [10]. Previous studies have demonstrated the successful use of durian peel extract in the synthesis of zinc oxide (ZnO) and silver (Ag) nanoparticles, both of which exhibited significant photocatalytic and antibacterial activities [11, 12]. However, despite TiO_2 being one of the most extensively studied photocatalysts, its green synthesis using durian peel extract has not yet been reported. This research gap highlights an opportunity for developing sustainable photocatalysts from agricultural waste.

This study focuses on synthesizing TiO_2 nanoparticles (TiO_2 NPs) via a sol - gel method assisted by durian peel extract as a green synthesis approach and evaluating their photocatalytic performance in dye degradation. The synthesis was conducted with variations in extract volume and synthesis pH. The crystal phase, band gap energy, particle size distribution, and surface charge properties of the resulting materials were determined. Indigo carmine was employed as a model organic dye pollutant to assess the photocatalytic activity of TiO_2 NPs under UV irradiation, with systematic variations in catalyst mass, dye concentration, and solution pH.

EXPERIMENTAL

Materials

Titanium IV isopropoxide (TTIP) from Sigma Aldrich 97 % was employed as the main precursor for TiO_2 and subsequently diluted in ethanol from Smart Lab and distilled water as solvents. Commercial TiO_2 (Merck) was also used for comparison. Durian peel (*Durio zibethinus*) was used as the source of the green synthesis bio - mediated extract. Indigo carmine dye (Sigma - Aldrich) was selected as the model organic pollutant without further purification. Hydrochloric acid (HCl, Merck) and sodium hydroxide (NaOH, Merck) were used for pH adjustment. Gallic acid (Merck) and quercetin (Merck) were used as standard references for determining TPC and TFC.

Preparation of the Durian peel extract

Durian peels were collected from a local market in Serpong, South Tangerang, and the white portion of the inner peel was carefully separated. The material was cut into small pieces, thoroughly washed, and dried at 60°C for 24 h. The dried peels were ground using a mechanical grinder and sieved through a 60 - mesh screen to obtain a fine powder. The powdered sample was then transferred into a glass flask with a foil - convered beaker and subjected to maceration using distilled water at a powder - to - solvent ratio of 1 : 10 (w/v). The extraction process was carried out under continuous stirring with a magnetic stirrer at 500 rpm and 80°C for

1 h. The resulting mixture was centrifuged at 7000 rpm for 5 min to separate the filtrate from the solid residue. The obtained filtrate was preserved under refrigeration and subsequently used as a stabilizing agent in the synthesis of TiO_2 nanoparticles [13]. The total phenolic content (TPC) was determined using the Folin - Ciocalteu method with gallic acid as a standard, whereas the total flavonoid content (TFC) was analysed using the $AlCl_3$ colorimetric method with quercetin as a standard [14].

Synthesis of TiO_2 NPs

TiO_2 NPs were synthesized via a green sol - gel method using durian peel extract as a natural stabilizing agent and titanium tetraisopropoxide (TTIP) as the precursor. A TTIP solution in ethanol (p.a) was hydrolysed by the gadual addition of distilled water and durian peel extract at a mixing ratio of TTIP: etanol: water: extract (2 : 5 : 1 : 1 v/v) under magnetic stirring at 500 rpm for 24 h at room temperature, as shown in (Fig. 1). The resulting gel was centrifuged at 9500 rpm for 8 min, washed dried 80°C for 24 h, calcined 500°C for 2 h, and ground to obtain white TiO_2. The volume of extract added to the TTIP solution with an initial pH of 5 was 2.5, 5, and 7.5 mL, denoted by the codes TiO_2 - A, TiO_2 - B, and TiO_2 - C. During synthesis with the optimal extracts, the initial pH was adjusted to 3, 5, 7, and 9, corresponding to TiO_2 -D, TiO_2 - A, TiO_2 - E, and TiO_2 -F, respectively. The pH was adjusted using HCl or

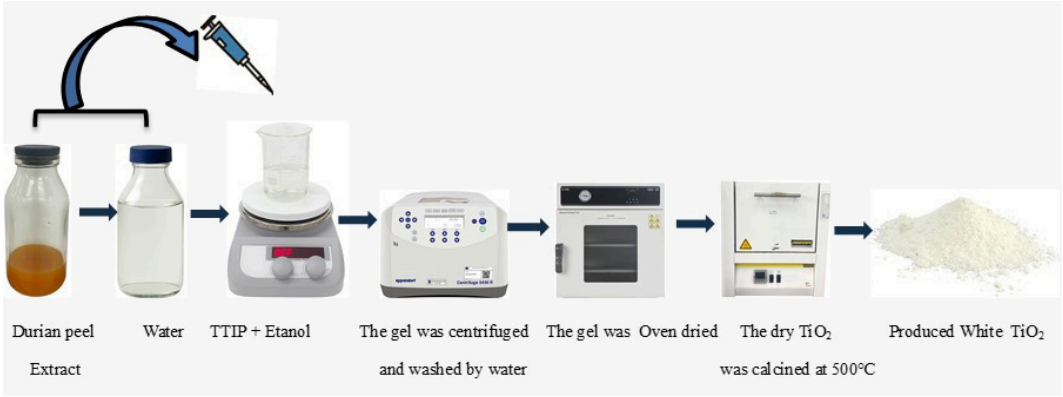

Fig. 1. Synthesis of TiO_2-NPs using durian peel extract.

NaOH. For comparison, commercial TiO_2 (Com - TiO_2) was used as a reference material [15].

Characterization of TiO_2 NPs

Functional groups were identified using Fourier transform infrared spectroscopy (FT - IR, Bruker Tensor II) in the range of 400 - 4000 cm^{-1}. The crystalline structure and phase of TiO_2 was analyzed using X - ray diffraction (XRD, Rigaku SmartLab, Cu Kα radiation (λ = 1.54 Å), and the average crystallite size was calculated using the Scherrer equation [16]. The particle size distribution was determined using a particle size analyser (Malvern Panalytical). Surface charge properties were evaluated by zeta potential analysis (Zetasizer Ultra, Malvern Panalytical). The optical bandgap was measured by UV - Vis diffuse reflectance spectroscopy (UV - Vis DRS) in the range of 200 - 400 nm.

Photodegadation experiment

The photocatalytic activity of TiO_2 was evaluated through indigo carmine degradation under UV irradiation. A 10 ppm dye solution was mixed with 0.1 g TiO_2 and pre - stirred in the dark for 15 min to establish adsorption - desorption equilibrium. The suspension was then irradiated with a UV lamp (λ = 254 nm, power = 20 watt) for 60 min. Then, 5 mL aliquots were withdrawn every 15 min, centrifuged at 10.000 rpm for 10 min, and analysed by UV - Vis spectrophotometry (Genesys 150 Thermo Scientific) at 500 - 700 nm. The degradation efficiency was calculated using Eq. (1).

$$\text{Degradation (\%)} = \frac{A_0 - A_t}{A_0} \times 100\ \% \qquad (1)$$

where A_0 is the initial indigo carmine absorbance and A_t is the absorbance at time [13]. The effects of catalyst dosage (0.1 - 0.4 g), initial dye concentration (5 - 40 ppm), and pH (3 - 9) were systematically investigated.

Reusability test

The reusability of TiO_2 was assessed under optimized experimental conditions, including the optimum catalyst dosage, initial indigo carmine concentration, and solution pH. The photocatalytic reactions were performed following the same procedure as the activity test. After each runs, the catalyst was recovered by vacuum membrane filtration, thoroughly washed by deionized waters, and dried at 80°C for 4 h before reuse. The photocatalytic performance stability was evaluated over four consecutive cycles [17].

RESULTS AND DISCUSSION

Total phenolic content (TPC) and total flavonoid (TFC) content of Durian peel

Table 1 presents the quantitative analysis of durian peel extract, showing a TPC of 43.68 mg GAE g^{-1} and a TFC of 27.95 QE g^{-1}. These values indicate a

Table 1. Total phenolic content (TPC) and total flavonoid (TFC) of durian peel extract.

Parameter	Value (mean ± SD)	unit
TPC (Total phenolic content)	43.68 ± 0.06	GAE g^{-1}
TFC (total flavonoid content)	27.95 ± 0.4	QE g^{-1}

high abundance of bioactive compounds with dual functionality as stabilizing agents in the green synthesis of TiO_2 nanoparticles. Phenolic compounds, through hydroxyl group, facilitate the stabilizing of titanium precursors and the formation Ti-O-Ti bond, whereas flavonoids interact with Ti^{4+} ions via hydroxyl and carbonyl groups, thereby preventing agglomeration and ensuring homogeneous nanoparticle dispersion [18].

Compared with other plant based extracts, such as green tea (*Camellia sinensis*, TPC 30 - 40 mg GAE g^{-1}) and mangosteen peel (*Garcinia mangostana*, TFC 50 - 60 mg QE g^{-1}), durian peel extract exhibits comparable phenolic and flavonoid contents [18 - 20]. This result suggests that the extract provides sufficient phytochemical strength to effectively mediate the sol-gel synthesis of TiO_2 nanoparticles. Moreover, the performance of nanocrystalline anatase with controlled particle growth is promoted.

Fourier transform infrared spectroscopy of the Durian peel extract and the prepared TiO_2

FT - IR spectroscopy was used to identify the functional groups present in the aqueous extract of durian peel and the synthesized TiO_2 nanoparticles. Fig. 2a, the extract exhibited characteristic absorption bands at 3303 cm^{-1} (O-H stretching of phenolics/flavonoids, typically observed in the 3200 - 3400 cm^{-1}) and 1632 cm^{-1} (C=O stretching and H-O-H bending of bound water, usually reported at 1600 - 1650 cm^{-1}), confirming the presence of secondary metabolites acting as capping agents. This result agrees with those of previous reports on polyphenol - mediated green synthesis [21].

After calcination at 500°C, significant spectral changes were observed in TiO_2 samples. At TiO_2 - B exhibited O-H (3612 cm^{-1}), C = O (1530 cm^{-1}) and Ti-O-Ti (502 cm^{-1}) bands were observed, indicating residual organic moieties coating the nanoparticle surface, consistent with the stabilizing role of phytochemicals [22]. In contrast TiO_2 - A showed a sharper spectrum dominated by the Ti-O-Ti vibration 516 cm^{-1}, suggesting that it is a purer TiO_2 with organic residues [23]. At higher extract volume TiO_2 - C the Ti-O-Ti vibration shifted to 503 cm^{-1}, which may be attributed to the effect of oxygen vacancies or bound water on lattice vibration [24].

The effect of pH was also evident **(**Fig. 2b**)**. At TiO_2 - D a dual band at 521 cm^{-1} and 502 cm^{-1} indicated heterogeneous Ti-O bonding due to limited phenolic deprotonation under acidic conditions [25]. At TiO_2 - E, the Ti-O-Ti band shifted to 529 cm^{-1} with the strongest intensity and minimal organic interference, reflecting a more stable and coordinated Ti-O-Ti network. Conversely, TiO_2 - F shifted to a lower wave number 506 cm^{-1}, suggesting weaker Ti-O bonds and higher defect densities caused by accelerated condensation [26]. Overall, the FT - IR spectra confirmed the role of durian peel extract as a dual capping agent. Furthermore, both extract volume and pH critically modulate Ti-

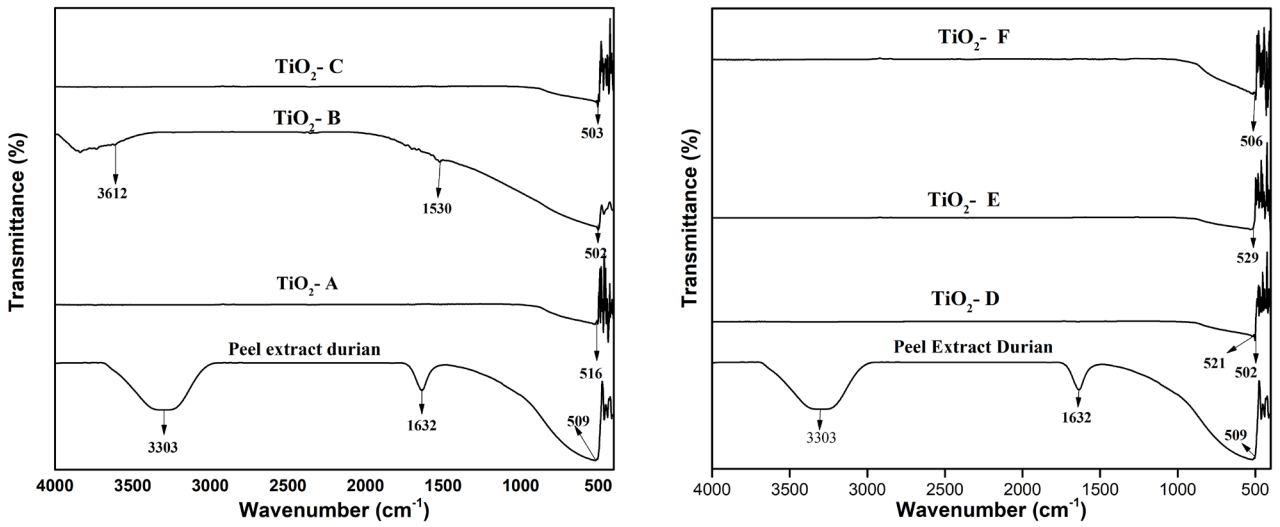

a) b)

Fig. 2. FT-IR spectrum of of Prepared TiO_2 (a) effect of extract volume and (b) effect of pH variation.

O-Ti network integrity, defect density, and surface chemistry. These structural modifications are expected to influence the photocatalytic activity, where stronger Ti-O-Ti coordination at TiO_2 - E correlates with higher crystallinity and potentially enhanced dye degradation.

X - Ray diffraction (XRD) analysis of prepared TiO_2 NPs

As shown in Fig. 3, XRD analysis confirmed that all TiO_2 samples synthesized via the sol - gel method with durian peel extract exhibited a pure anatase phase, consistent with JCPDS 96 - 900 - 9088, with the main diffraction peak at (101) around 25° [27, 28]. Calcination at 500°C successfully produced stable anatase crystals without rutile or brookite impurities.

Peak broadening indicated a progressive reduction in the crystallite size with increasing extract volume and under more alkaline conditions. Scherrer calculations (Table 2) revealed that the crystallite sizes ranged from 9.15 nm (TiO_2 - A) to 5.79 nm (TiO_2 - F), which was significantly smaller than commercial TiO_2 48.41 nm. This demonstrates the role of organic metabolites as capping agents that inhibit crystal growth and promote nucleation, thereby yielding nanoscale particles [29].

The XRD findings correlate well with the FT - IR results. At TiO_2 - B, residual O-H (3612 cm^{-1}) and C=O (1530 cm^{-1}) bands supported the presence of organic compound, consistent with smaller crystallite sizes. In contrast, TiO_2 - A exhibited a dominant Ti-O-Ti band (516 cm^{-1}), reflecting purer TiO_2 with slightly larger crystals due to minimal capping influence. At TiO_2 -

Table 2. Crystallite Sizes of prepared TiO_2.

Sample	Crystallite size, nm
TiO_2 - A	9.15
TiO_2 - B	7.80
TiO_2 - C	6.80
TiO_2 - D	9.06
TiO_2 - E	7.41
TiO_2 - F	5.79
Com - TiO_2	48.41

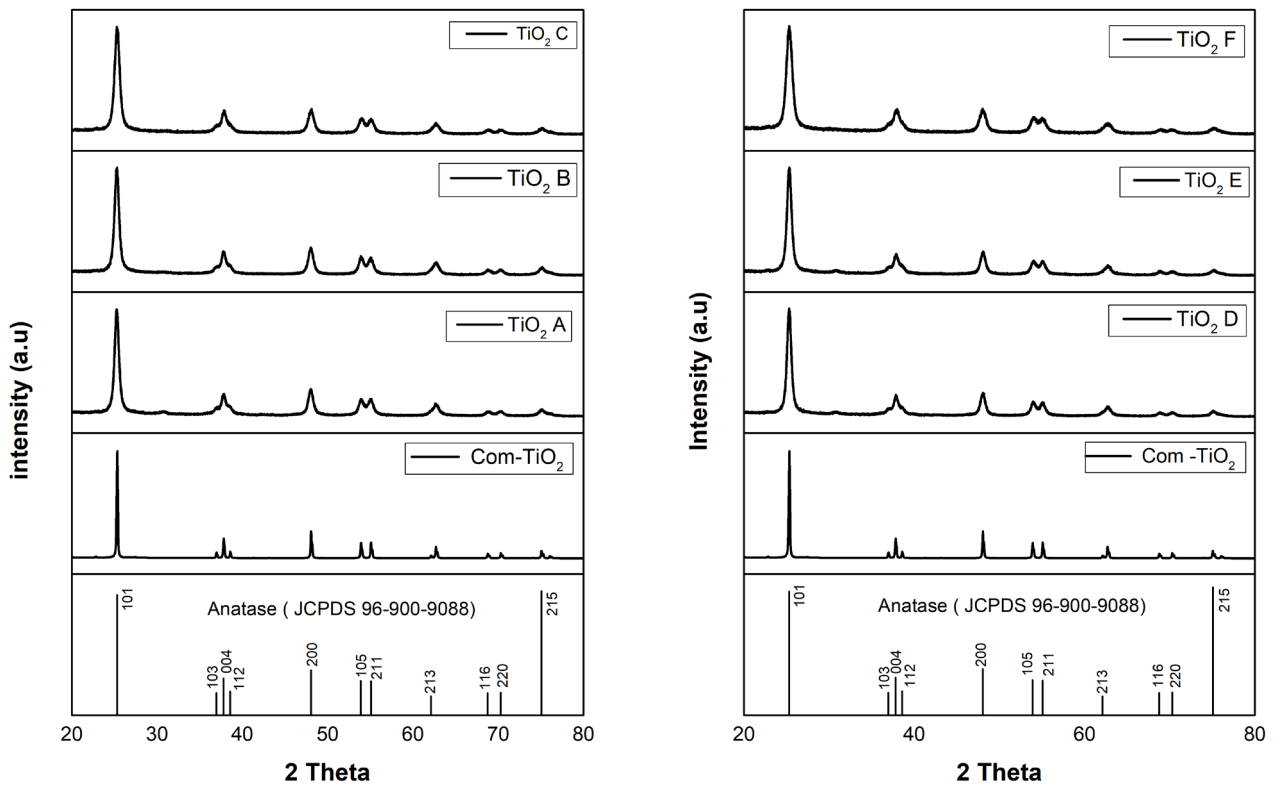

Fig. 3. XRD pattern of prepared TiO_2 (a) effect of extract volume and (b) effect of pH variation.

C the Ti-O-Ti shift to 503 cm^{-1} may indicate oxygen vacancies, aligning with the smallest crystallite size. pH effects further validated this relationship. TiO_2 - D, heterogeneous Ti-O bonding (521 or 502 cm^{-1}), showed relatively larger crystallites, while TiO_2 - E correlated exhibited strong Ti-O-Ti bonding at 529 cm^{-1} with intermediate crystallite size, suggesting optimal structural order. Conversely, TiO_2 - F exhibited lower wavenumber shifts, signifying weakened Ti-O bonds and higher defect density, consistent with the smallest crystallites resulting from accelerated condensation [26]. Compared with other plant - mediated syntheses, the crystallite size obtained in this work is notably smaller. For example, TiO_2 NPs synthesized using mangosteen extract typically range from 12 to 15 nm [30], and green tea peel extract approximately 21.04 nm [18]. The smaller crystallite sizes achieved with durian peel extract highlight its superior capping efficiency, which is attributed to its high polyphenol and flavonoid content.

Smaller crystallite sizes are generally advantageous from an application perspective because they provide a larger specific surface area, offering more active sites for dye degradation. Oxygen vacancies and defect states, while potentially enhancing dye adsorption, may also increase electron - hole recombination rates. Therefore, balancing the crystallite size and structural defects is critical for optimizing the photocatalytic activity of the resulting TiO_2 nanoparticles [31].

Particle size analyzer and zeta potential of prepared TiO_2 NPs

PSA measurement demonstrated that both extract volume and synthesis pH strongly influenced particle size. As shown in Fig. 4. increasing the extract volume caused a non - linear trend, with the hydrodynamic diameter increasing from 86.2 nm (TiO_2 - A) to 101.9 nm (TiO_2 - B) and 27.9 nm (TiO_2 - C). This data suggests that incomplete surface capping allowed agglomeration at moderate extract volume, whereas excess extract provided stronger phenolic/flavonoid capping, effectively minimizing aggregation and leading to ultra-small hydrodynamic sizes. For comparison, commercial TiO_2 exhibited a hydrodynamic particle size of 233.6 nm, which is significantly larger than that of the biosynthesized TiO_2 samples. This indicates that the green synthesis approach using plant extract effectively produces nanoparticles with smaller size and better dispersion stability than commercial TiO_2.

Variation in pH also showed a significant effect on particle size, with values of 120 nm for TiO_2 - D at pH 3, 81.4 nm for TiO_2 - E at pH 7, and 103.2 nm for TiO_2 - F at pH 9. For comparison, TiO_2 - A at pH 5 exhibited a particle size of 86.2 nm. These results clearly indicate that under neutral (pH 7) and slightly acidic (pH 5) conditions, the particle size tends to be smaller than that in strongly acidic (pH 3) or alkaline (pH 9) environments. These values are substantially larger than the XRD crystallite size, reflecting the hydrodynamic diameter of agglomerated particles surrounded by solvated organic shells [32]. Increased extract volumes enhanced phenolic/flavonoid capping, thereby restricting crystal growth, whereas alkaline conditions promoted agglomeration and neutral pH favored controlled nucleation [33, 34]. A similar observation was reported for TiO_2 synthesized using *Sizygium cumini* seed extract, which showed a hydrodynamic size of 120 nm despite much smaller XRD crystallited, confirming that particle agglomeration and solvated organics typically enlarge the measured diameter [35].

Zeta potential analysis (Fig. 5) showed values ranged from - 32.0 mV (TiO_2 - A) to - 23.1 mV (TiO_2 - B) and - 20.13 mV (TiO_2 -C). After pH adjustment, the values shifted - 32.7 mV (TiO_2 - D) to - 29.0 (TiO_2 - E) and finally - 25.1 mV (TiO_2 - F). The commercial TiO_2 exhibited a zeta potential of - 25.32 mV, indicating moderate electrostatic stability. Zeta potentials above ± 30 mV indicated strong electrostatic stability, whereas lower magnitudes suggest moderate stability [36]. The shift toward negative charge is consistent with the point of zero charge pH pzc, as the TiO_2 surface tends to be negatively charged at pH > pHpzc. This observation agrees with a previous report on the synthesis of TiO_2 using *Ocimum sanctum* leaf extract, where negative zeta potentials demonstrated good nanoparticle surface stability [37]. For neem extract -mediated TiO_2, smaller particles improved the surface area but reduced the zeta potential, which lies between size minimization (enhancing surface active sites) and colloidal stability (ensuring effective dye dispersion) [38].

In summary, particle size minimization was achieved at TiO_2 - C, whereas the highest electrostatic occurred at TiO_2 - D. This underscores the trade-off between the reduction of crystallite size and colloidal stability. Comparable findings were noted in [39].

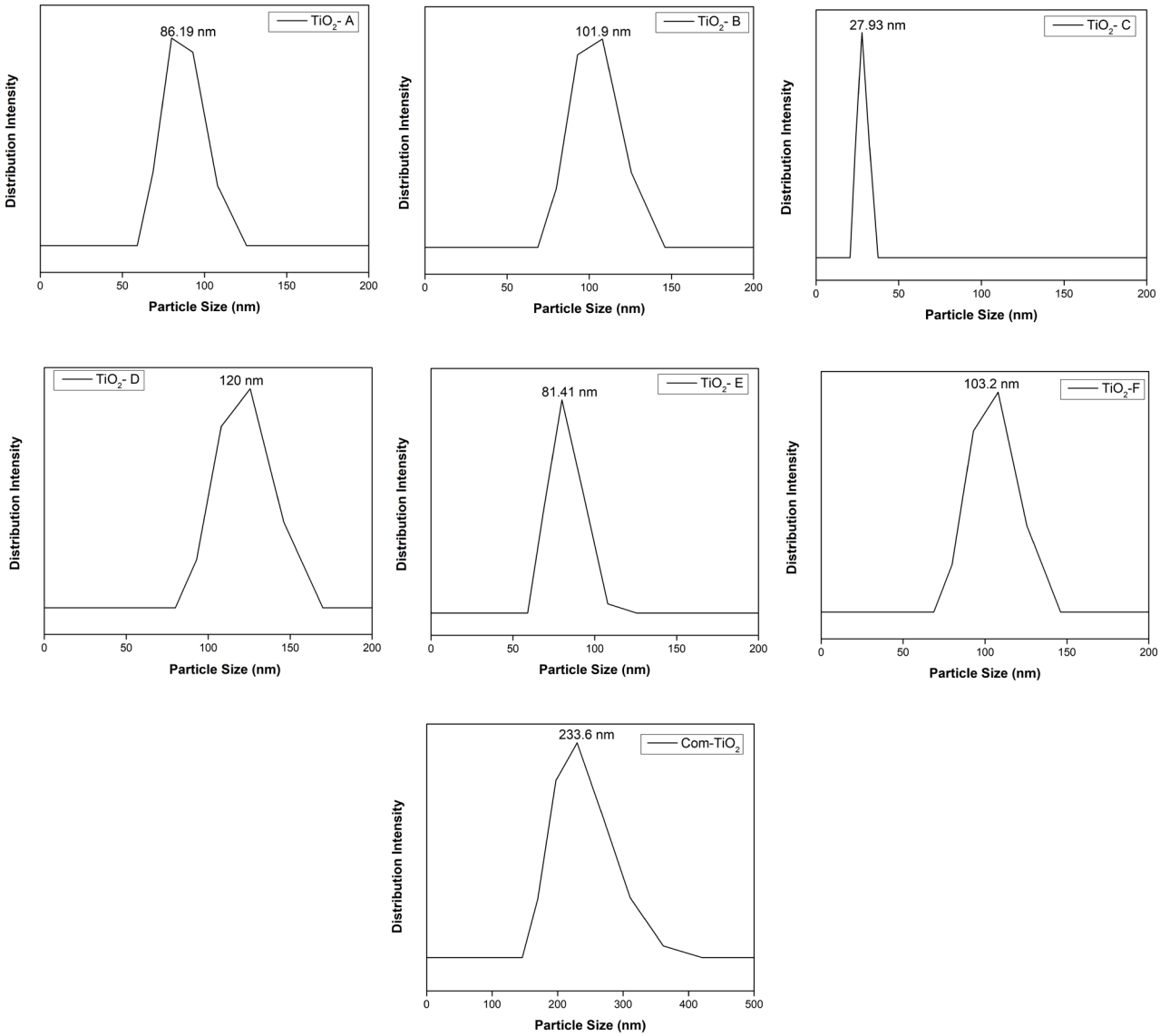

Fig. 4. Particle size of the prepared TiO_2.

Ultraviolet - visible diffuse reflectance spectroscopy (UV- Vis DRS)

UV- Vis DRS analysis the Kubelka Munk (Tauch Plot) method revealed bandgap values of 3.23 - 3.29 eV for TiO_2 nanoparticles synthesized using the durian peel extract. Variation in extract volume yielded **(**Fig. 6a**)** 3.23 eV (TiO_2 - A), 3.26 eV (TiO_2 - B), and 3.27 eV (TiO_2 - C), while pH variation produced 3.29 eV (TiO_2 - D), 3.25 eV (TiO_2 - E), and 3.29 eV (TiO_2 - F). These values are consistent with anatase TiO_2 bandgap (3.27 eV) reported in the literature [40, 41].

Correlation with PSA and zeta potential indicates that higher extract volumes reduce particle size, thereby enhancing surface passivation and slightly shifting the band gap upward, likely due to increased surface electron density influenced by organic ligands [42]. At extreme pH (TiO_2 -C and TiO_2 - D), the excess protonation of phenolics provides stronger coordination with Ti centers. Both effects help preserve higher bandgaps (3.29 eV). Conversely, near - neutral TiO_2 - E exhibited the lowest bandgap (3.25 eV), while TiO_2 - A showed an even smaller band gap of 3.23 eV [43]. This can be associated with residual organic molecules introducing mid - gap or sub -band states that facilitate additional light absorption [44, 45]. Overall, bandgap TiO_2 synthesized with durian peel extract shows good agreement with commercial

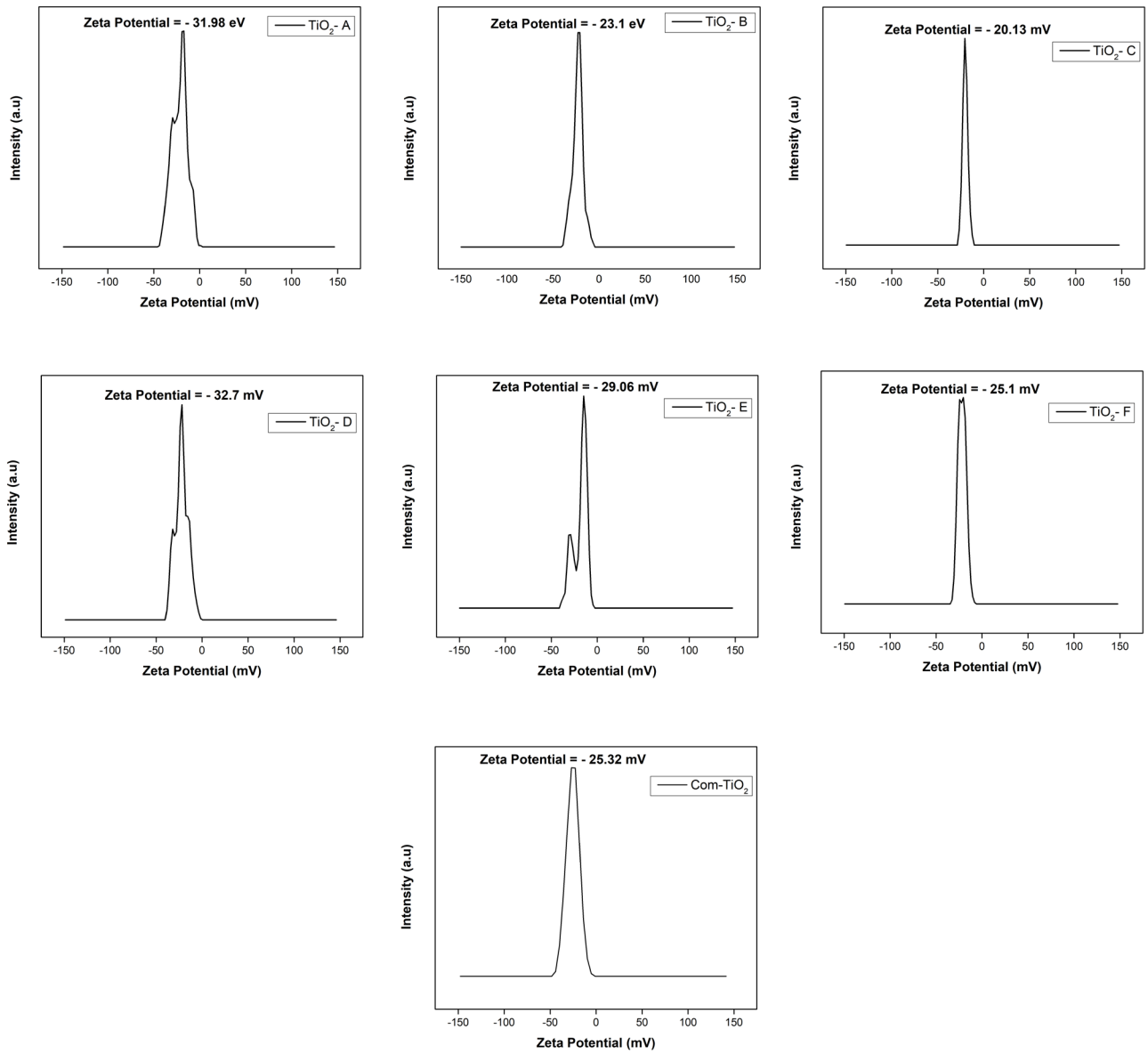

Fig. 5. Zeta potential of the prepared TiO_2.

anatase, confirming the optical suitability of this green synthesized material for photocatalytic applications.

Photocatalytic activity of the prepared TiO_2 NPs

The direct photolysis of indigo carmine was inefficient, achieving only 17 % degradation after 60 min, highlighting the need for a photocatalyst [46, 47]. In contrast, TiO_2 synthesized with durian peel extract (Fig. 7a) (TiO_2 A - C) exhibited markedly higher activity, degrading > 60 % of dye within 15 min and reaching nearly 100 % within 60 min, whereas commercial TiO_2 remained slower (30 % at 15 min). The superior performance of extract - mediated TiO_2 can be attributed to the smaller crystallite size (6 - 9 nm), which increases the density of surface-active sites and induces a slight bandgap widening (3.23 eV). This structural optical synergy promotes more efficient electron–hole separation, enhancing photon absorption and the generation of reactive oxygen species (ROS) such as •OH and $•O_2^-$ radicals responsible for dye

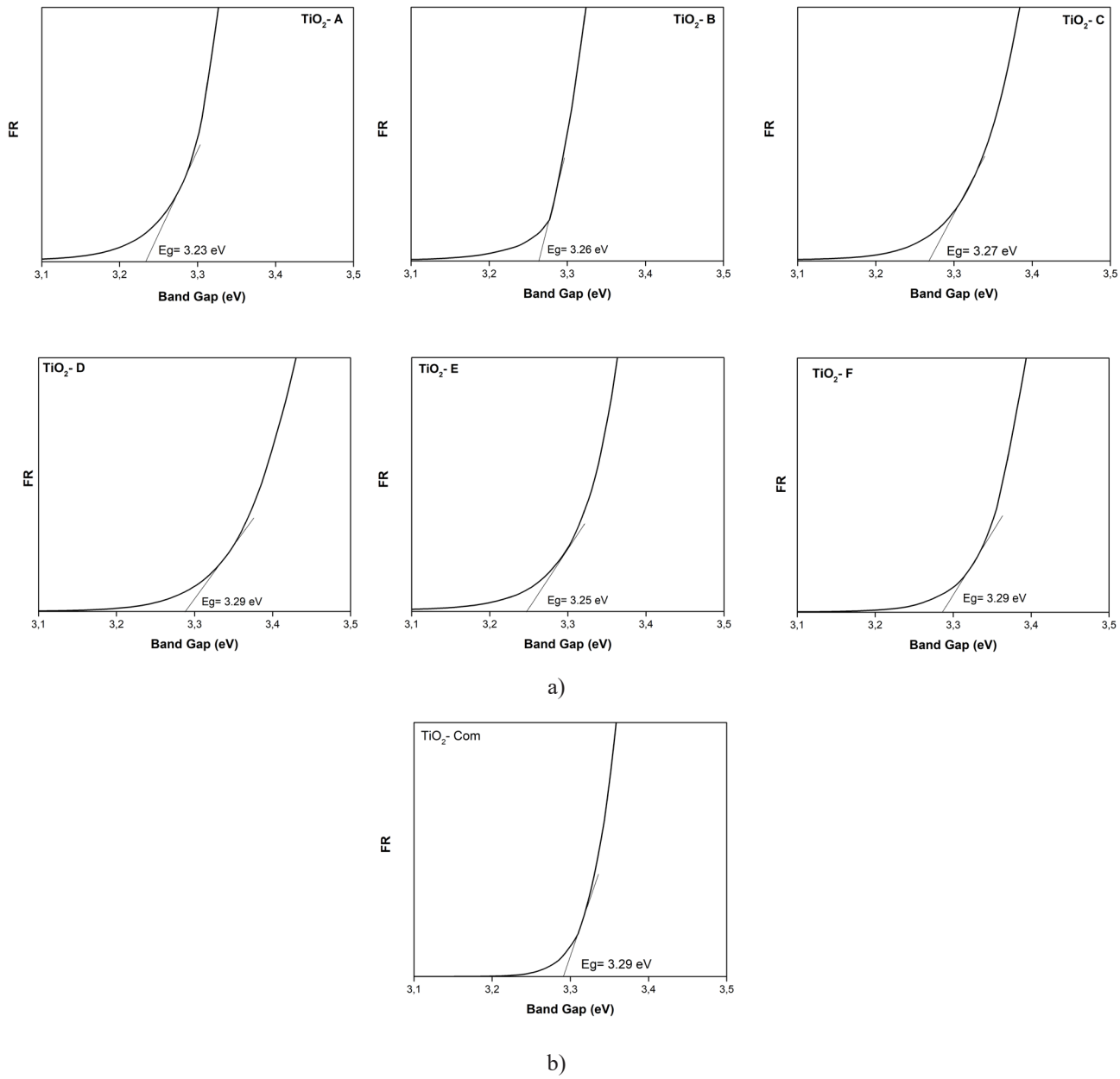

a)

b)

Fig. 6. (a) Bandgap value of the synthesized TiO_2 nanoparticles based on the Kubelka-Munk factor plot. (b) Bandgap value of commercial TiO_2.

mineralization [48]. This is consistent with recent studies reporting that the reduction of TiO_2 crystallite size facilitates charge separation and increases ROS productivity, which directly enhances photocatalytic performance [31].

The effect of synthesis pH is also critical. Catalysts prepared at pH 3 - 7 (Fig. 7b) achieved nearly 100 % degradation within 60 min, whereas those prepared at pH 9 decreased to 90 % degradation. Although alkaline synthesis promoted smaller crystallites, the strongly negative surface charge at pH > pH pzc = 4.32 induced electrostatic repulsion with anionic dye molecules, thereby suppressing adsorption and limiting photocatalytic activity [49]. Therefore, TiO_2 - D was selected as photocatalyst for further experiment.

The initial dye concentration significantly influenced the degradation percentage. At 5 - 10 ppm (Fig.8b), nearly complete degradation was achieved within 60 min, whereas higher concentrations 30 - 40 ppm reduced efficiency to 60 - 70 %. This decline is consistent with

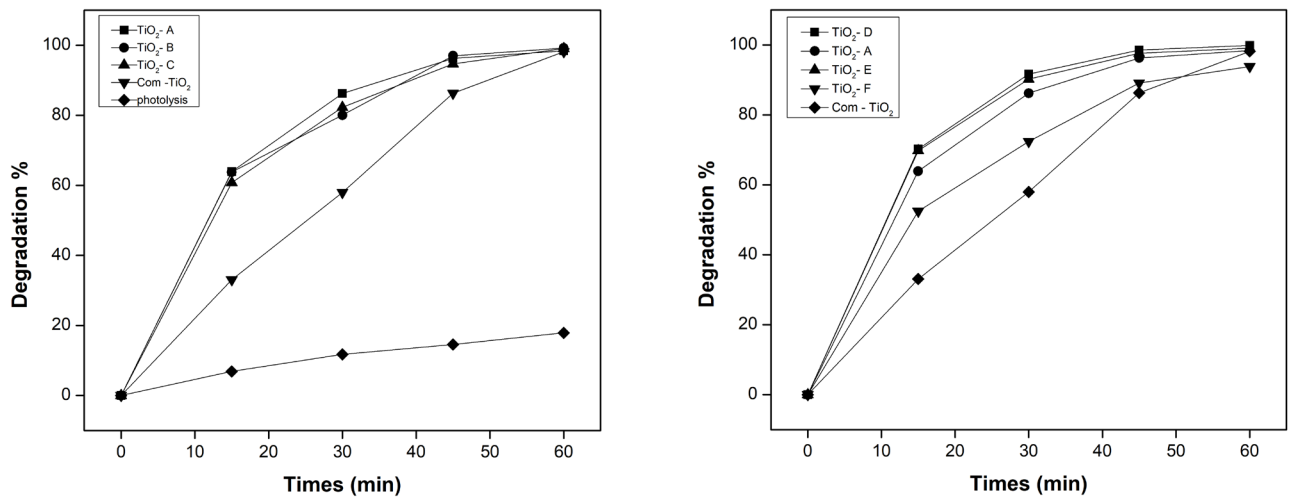

Fig. 7. Degradation efficiency of indigo carmine using prepared TiO_2: (a) effect of extract volume and (b) effect of synthesis pH.

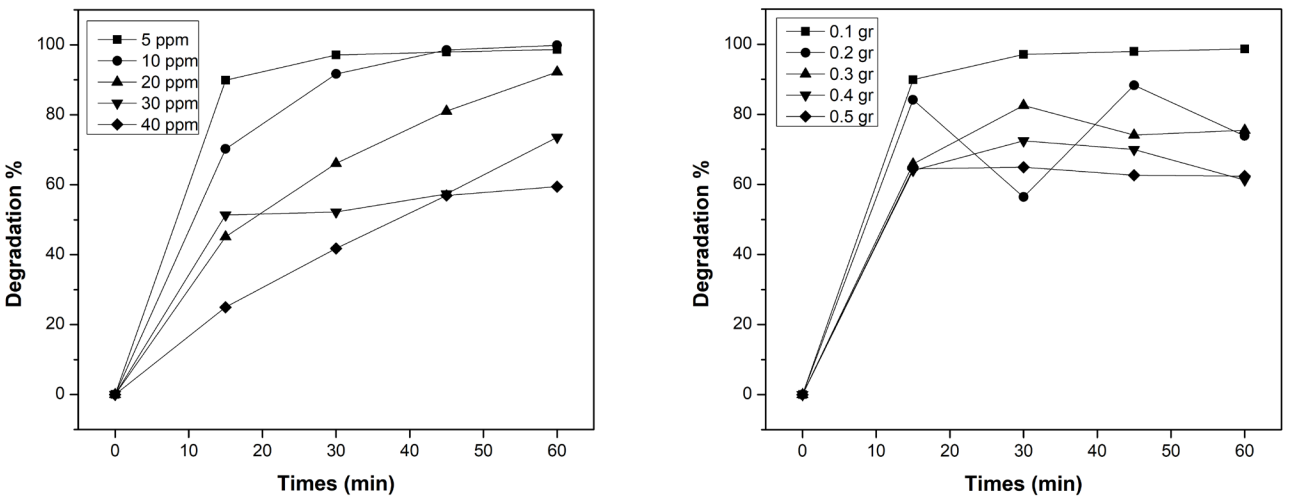

Fig. 8. Degradation percentage of indigo carmine using prepared TiO_2-D: (a) effect of mass catalyst and (b) effect of initial dye concentration.

the Langmuir Hinshelwood kinetic model, where increasing the dye concentration saturates the catalyst surface and decreases the apparent rate constant k due to reduced •OH radical availability [50, 51]. The catalyst loading also demonstrated an optimum. Maximum efficiency was achieved at 0.1 g (Fig. 8a), but higher dosages reduced performance due to excessive light scattering and opacity, which limit photon penetration and consequently suppress ROS [52, 53].

The solution pH further modulated the photocatalytic efficiency. Under acidic conditions (Fig. 9) (pH < pH pzc = 4.32), the electrostatic attraction between the positively charged TiO_2 surface and the anionic dye molecules enhanced the adsorption and accelerated the degradation. This result was supported by zeta potential data (-32.7 mV at TiO_2 - D), which indicated strong colloidal stability and favourable dye catalyst [54].

Overall, the green - synthesized TiO_2 derived from durian peel extract exhibits superior photocatalytic performance compared to commercial TiO_2, with optimal activity under acid to neutral pH, low dye concentrations, and moderate catalyst loading. The system achieved nearly complete indigo carmine degradation within 60 min under UV - irradiation. According to a previous report, the photocatalytic oxidation of indigo carmine predominantly proceeds via cleavage of the central C=C

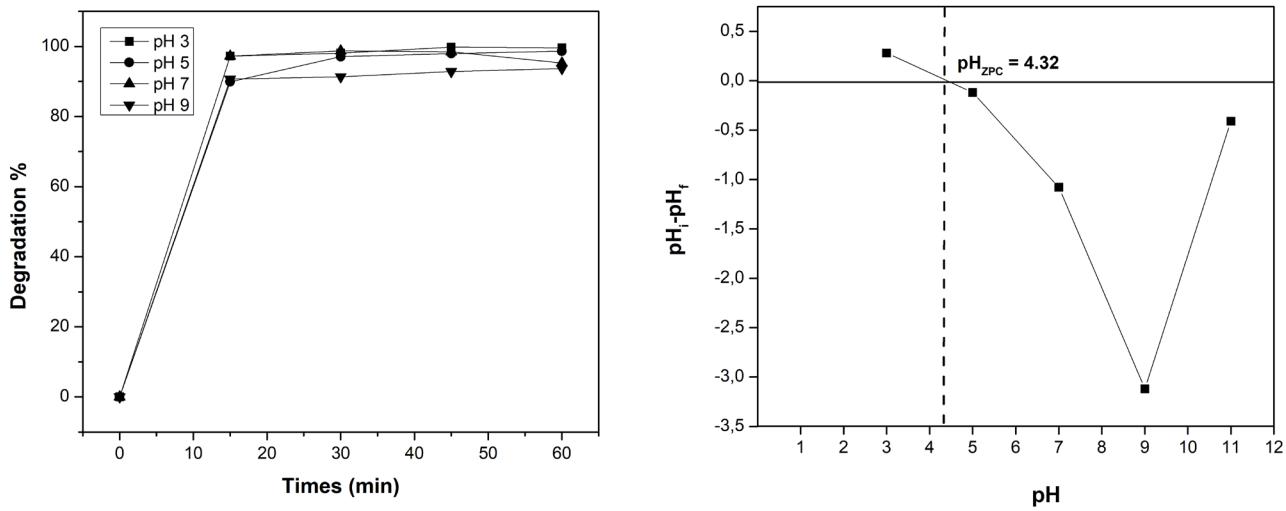

Fig. 9. Degradation percentage of indigo carmine using prepared TiO_2-D (a) Point of zero charge TiO_2-D (b) Effect of dye pH.

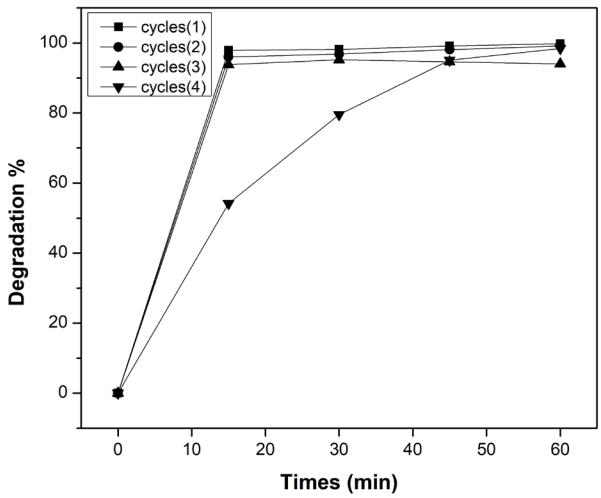

Fig. 10. Reusability of TiO_2-D as a photocatalyst for indigo carmine degradation.

bond followed by desulfonation of the -SO^- group, yielding sulfonated aromatic intermediates such as isatin-5-sulfonic acid and 2-amino-5-sulfobenzoic acid before final mineralization into CO_2, NO_3^-, and SO_4^{2-} [55].

Reusability of the prepared TiO_2 catalyst

Reusability tests of TiO_2 - D in indigo carmine degradation demonstrated stable performance over three cycles, maintaining nearly 100 % efficiency (Fig.10). A slight decline of 98.41 % was observed in the fourth cycle, accompanied by a catalyst mass loss of 0.03 g from the initial 0.10 g, corresponding to a 30 % reduction. The decrease can be attributed to unavoidable catalyst loss during recovery and washing. These findings confirm the good reusability of TiO_2 based photocatalysts, consistent with reports that activity may gradually decline due to mass loss over repeated use [56, 57].

CONCLUSIONS

TiO_2 nanoparticles were successfully synthesized via a green sol - gel route using durian peel extract as a natural stabilizer agent, yielding pure anatase with a crystallite size 5 - 10 nm, a band gap of 3.23 - 3.29 eV, and good colloidal stability. The photocatalyst exhibited outstanding efficiency, achieving ± 99 % degradation of indigo carmine within 60 min and maintaining nearly 100 activities over three reuse cycles using TiO_2 - D as photocatalyst. These findings highlight the potential of durian peel as a sustainable green stabilizer that supports circular economy practices. However, further studies on real wastewater matrices and long - term recyclability are required for industrial implementation.

Acknowledgments

This work was supported by the Indonesia Endowment Fund for Education Agency through the Research and Innovation Program for Advanced Indonesia Competition (RIIM - competition G7), National Research and Innovation Agency (BRIN, Grant No. B-3871/II.7.5/KS.00/4/2025 and B-2599/III.10/FR.06.00/4/2025).

Authors' contributions

D.N.S.: Experimental work, Writing original draft, Formal analysis, Design of research; K.K.: Conceptualization, Methodology, Validation, Formal analysis, Writing - review & Editing, Design of the research, Project management and funding acquisition; R.D.Y.: Writing - review & Editing and Validation; A.H., R.A.P., V.S, and T.O: Formal analysis and Validation.

REFERENCES

1. R. Al-Tohamy, S.S. Ali, F. Li, K.M. Okasha, Y.A.G. Mahmoud, T. Elsamahy, A critical review on the treatment of dye-containing wastewater: Ecotoxicological and health concerns of the textile dyes and possible remediation approaches for environmental safety, Ecotoxicol. Environ. Saf., 231, 2022, 1-17.
2. M.E. Ristea, O. Zarnescu, Effects of indigo carmine on growth, cell division, and morphology of Allium cepa L. root tip, Toxics, 12, 3, 2024, 1-14.
3. T. Kekes, C. Tzia, Adsorption of indigo carmine on functional chitosan and β- cyclodextrin/chitosan beads: Equilibrium, kinetics and mechanism studies, J. Environ. Manage., 370, 2024, 1-11.
4. Y. Liu, J. Chen, D. Duan, Z. Zhang, C. Liu, W. Cai, Environmental impacts and biological technologies toward sustainable treatment of textile dyeing wastewater: A review, Sustainability, 16, 2024, 1-23.
5. D. Patel, A. Singh, S.R. Ambati, R.S. Singh, R.K. Sonwani, On overview of recent advances in treatment of complex dye-containing wastewater and its techno-economic assessment, J. Environ. Manage., 370, 2024, 1-23.
6. T.A. Aragaw, F.M. Bogale, Role of coagulation/flocculation as a pretreatment option to reduce colloidal/bio-colloidal fouling in tertiary filtration of textile wastewater: A review and future outlooks, Front. Environ. Sci., 11, 2023, 1-16.
7. A. Chakravorty, S. Roy, A review of photocatalysis, basic principles, processes, and materials, Sustain. Chem. Environ., 8, 2024, 1-18.
8. D.R. Eddy, D. Rahmawati, M.D. Permana, T. Takei, Solihudin, Suryana, A.R. Noviyanti, I. Rahayu, A review of recent developments in green synthesis of TiO_2 nanoparticles using plant extract: Synthesis, characterization and photocatalytic activity, Inorg. Chem. Commun., 165, 2024, 1-12.
9. I.S. Afonso, B. Cardoso, G. Nobrega, G. Minas, J.E. Ribeiro, R.A. Lima, Green synthesis of nanoparticles from olive oil waste for environmental and health applications: A review, J. Environ. Chem. Eng., 12, 2024, 1-20.
10. A. Wisetsai, L. Tabtimmai, C. Sonklin, A. Joompang, N. Srisukpachin, S. Jadsadajerm, S. Preepram, Photoprotective property, bioctivities, and chemical composition of durian peel extracts: Agricultural waste valorization for cosmetic and pharmaceutical applications, Nat. Resour. Human Health., 5, 3, 2025, 449-461.
11. T.D. Nguyen, N.M. Pham, N.T. T. Thai, H.T. T. Nguyen, Y.H. Hoang, A.C. Ha, Characterization and applications of silver nanoparticles photosynthesized from Durio zibethinus peel extract, Biointerface Res. Appl. Chem., 14, 5, 2024, 1-15.
12. V. Ravichandran, S. Sumitha, C.Y. Ning, O.Y. Xian, U. K. Yu, N. Paliwal, S. A. A. Shah, M. Tripathy, Durian waste mediated green synthesis of zinc oxide nanoparticles and evaluation of their antibacterial, antioxidant, cytotoxicity and photocatalytic activity, Green Chem. Lett. Rev., 13, 2, 2020, 102-116.
13. A.B. Aritonang, R.A. Putri, V. Sisca, M.J. Madiabu, K. Khoiriah, Photocatalytic degradation of acid Yellow 25 using nanoparticle TiO_2 mediated petai pod extract, Baghdad Sci. J., 22, 6, 2025, 1851-1862.
14. K.R.P. Sari, Z. Ikawati, R. Danarti, T. Hertiani, Micro-titer plate assay for measurement of total phenolic and total flavonoid contents in medicinal plant extracts, Arab. J. Chem., 16, 2023, 1-8.
15. K. Khoiriah, R.A. Putri, Biosynthesis of titanium dioxide nanoparticles using peel extract of parkia speciosa for methyl orange degradation, S. Afr. J. Bot., 170, 2024, 120-129.
16. M.S. Mohtaram, S. Mohtaram, S. Sabbaghi, X. You, W. Wu, L. Jia, K. Muzammil, N.A. Alraee, S. Islam, Y. Aryanfar, Photocatalytic degradation of acetaminophen using a novel TiO_2 -orange peel- derived biochar composite: Synthesize, characterization and optimization of key factors, J. Water Process Eng., 58, 2024, 1-13.
17. D. Kanakaraju, P.P. Natashya, Y.C. Lim, I. A. W. Tan, Functionalized TiO_2-wasted-derived photocatalytic materials for emerging pollutant degradation: synthesis and optimization, Environ. Monit. Assess.,

197, 2025, 1-22.
18. T.K.N. Tran, L.K.V. Tran, N.C.T. Vo, T.Q.M. Doan, H.D. Pham, T.N.D. Ngyen, Green synthesis of titanium dioxide nanoparticles using green tea (Camellia sinensis) extract: Characteristics and applications, Green Process. Synth., 14, 2025, 1-15.
19. V. Rocha, P. Ferreira-Santos, C. Aguiar, I.C. Neves, T. Tavares, Valorization of plant by-products in biosynthesis of silver nanoparticles with antimicrobial and catalytic properties, Environ. Sci. Pollut. Res., 31, 2024, 14191-14207.
20. T.P. Vo, N.D. Pham, T.V. Pham, H.Y. Nguyen, L.T.V. Vo, T.N.H. Tran, T.N. Tran, D.Q. Nguyen, Green extraction of total phenolic and flavonoid contents from mangosteen (Garcinia mangostana L.) rind using natural deep eutectic solvents, Heliyon., 9, 2023, 1-13.
21. Deliza, S.L. Rahayu, A.R. Liandi, R.A. Putri, S. Safni, Green synthesis approach on fabrication of TiO_2 nanoparticle using peel extract of Baccaurea recemosa for photocatalytic degradation of Acid Red - 185, Environ. Nanotechnol. Monit. Manage., 23, 2025, 1-10.
22. D. Rahmawati, M. D. Permana, D.R Eddy, N. Saito, T. Takei, Suryana, A. R. Noviyanti, I. Rahayu, M. H. Helal, Z. M. El-Bahy, Synthesis of TiO_2 nanoparticles using red spinach leaf extract (Amaranthus tricolor) for photocatalytic of methylene blue degradation, Green Chem. Lett. Rev., 17, 1, 2024, 1-13.
23. H. Sellami, M.O. Akinyemi, M. Gdoura-Ben Amor, D.C. Onwudiwe, D.M.N. Mthiyane, Structural and optical characterization of TiO_2 nanoparticles synthesized using Globularia alypum leaf extract and the antibacterial properties, Discov. Appl. Sci., 7, 2025, 1-19.
24. N. Sofyan, Y. Rilda, Andriayani, F. Angellinnov, M. M'rad, Muhammad, A. Ridhova, A.H. Yuwono, D. Dhaneswara, Sustainable synthesis of TiO_2 nanoparticles from gambier leaf extract for enhanced DSCC photocurrent response, Results Mater., 27. 2025, 1-14.
25. M.E. Simonsen, E.G. Søgaard, Sol-gel reactions of titanium alkoxides and water: influence of pH and alkoxy group on cluster formation and properties of the resulting products, J. Sol-Gel Sci. Technol., 53, 3, 2010, 485-497.
26. N. Khima, A. Chelouche, F. Challali, D. Djouadi, A. Djermoune, M. Luce, A. Cricenti, D. Becerril, S. Bellucci, T. Touam, TiO_2 sol-gel thin films: effect of acidic and basic PH on physical characteristics, J. Sol-Gel Sci. Technol., 112, 2024, 277-288.
27. H.F. Oleiwi, A.J. Rahma, S.I. Salih, A.A, Beddai, Comparative study of sol-gel and green synthesis technique using orange peel extract to prepare TiO_2 nanoparticles, Baghdad Sci. J., 21, 5, 2024, 1702-1711.
28. M.V. Arularasu, Effect of organic capping agents on the optical and photocatalytic activity of mesoporous TiO_2 nanoparticles by sol-gel methond, SN Appl. Sci., 1, 2019, 393.
29. A. Verma, R. K. Sharma, S. Kumar, Influence of synthesis parameters on structural and optical properties of sol-gel derived TiO_2 nanoparticles, Mater. Today Proc., 45, 2021, 1234-1239.
30. E.-Y. Ahn, S.-W. Shin, K. Kim, Y. Park, Facile green synthesis of titanium dioxide nanoparticles by upcycling mangosteen (Garcinia mangostana) pericarp extract, Nanoscale Res. Lett., 17, 2022, 1-12.
31. D. Li, H. Song, X. Meng, T. Shen, J. Sun, W. Han, X. Wang, Effects of particle size on the structure and photocatalytic performance by alkali- treated TiO_2, Nanomaterials, 10, 3, 2020, 1-14.
32. S.K. Filippov, R. Khusnutdinov, A. Murmiliuk, W. inam, L. Ya. Zakhrova, H. Zhang, V. . Khutoryanskiy, Dynamic light scattering and transmission electron microscopy in drug delivery: a roadmap for correct characterization of nanoparticles and interpretation of results, Mater. Horiz., 10, 2023, 5354-5370.
33. A. Azad, H. Zafar, F. Raza, M. Sulaiman, Factors influencing the green synthesis of metallic nanoparticles using plant extracts: A comprehensive Review, Pharm. Front., 5, 3, 2023, e117-e131.
34. C. Guiot, O. Spalla, Stabilization of TiO_2 nanoparticles in complex medium through a PH adjustment protocol, Environ. Sci. Technol., 47, 4, 2013, 2049-2056.
35. M. Rayzah, A.Y. Elderdery, N.A.N. Alzerwi, B. Alzahrani, A. Alsrhani, A. Alsultan, B. Idrees, F. Rayzah, Y. Bakhsh, A.M. Alzahrani, S.K. Subbiah, P.L. Mok, Syzygium cumini (L.) extract derived green titanium dioxide nanoparticles induce caspase-dependent apoptosis in hepatic cancer cells, Plants, 12, 18, 2023, 1-16.
36. Z. Nemeth, I. Csoka, R. Semnani Jazani, B. Sipos, H. Haspel, G. Kozma, Z. Konya, D.G. Dobo, Quality by design- driven zeta potential optimisation study of liposomes with charge imparting membrane additives, Pharmaceutics, 14, 2022, 1-25.

37. M.Z. Ahmad, A.S. Alasiri, J. Ahmad, A.A. Alqahtani, M.M. Abdullah, B.A. Abdel- Wahab, K. Pathak, R. Saikia, A. Das, H. Sarma, S.A. Alzahrani, Green synthesis of titanium dioxide nanoparticles using Ocimum sanctum leaf extract: in vitro characterization and its healing efficacy in diabetic wounds, Molecules, 27, 2022, 1-17.
38. M. Saeed, M. Muneer, M.K.K. Khosa, N. Akram, S. Khalid, M. Adeel, A. Nisar, S. Sherazi, Azadirachta indica leaves extract assisted green synthesis of Ag-TiO_2 for degradation of methylene blue and Rhodamin B dyes in aqueous medium, Green Process Synth., 8, 2019, 659-666.
39. P. Mohanasundram, M.S.A., In vitro scratch assay, cytotoxicity, DNA/BSA binding properties, and antimicrobial activity of green synthesized TiO_2 nanoparticles via neem flowers, Mater. Adv., 6, 2025, 3533-3545.
40. G. Nabi, W. Raza, M.B. Tahir, Green synthesis of TiO_2 nanoparticle using cinnamon powder extract and study of optical properties, J. Inorg. Organomet. Polym. Mater., 30, 2020, 1425-1429.
41. S. Valencia, J.M. Marin, G. Restrepo, Studi of the bandgap of synthesized titanium dioxide nanoparticules using the sol-gel method and a hydrothermal treatment, Open Mater. Sci. J., 4, 2010, 9-14.
42. S. Wahyuningsih, I. Kartini, A.H. Ramelan, L.N.M.Z. Saputri, H. Munawaroh, Band- engineering of TiO_2 as a wide-band gap semiconductor using organic chromophore dyes. IOP Conf. Ser. Earth Environ. Sci., 75, 2017, 1-9.
43. C.A. D'Amato, R. Giovannetti, M. Zannotti, E. Rommozzi, M. Minicucci, R. Gunnella, A. Di Cicco, Band gap implications on nano-TiO_2 suface modification with ascorbic acid for visible light active polypropylene coated photocatalyst, Nanomaterials, 8, 2018, 1-14.
44. R. Sarathi, S. Meenakshi Sundar, Effect of pH variation on band gap and visible light photocatalytic properties of TiO_2 nanoparticles, J. Water Environ. Nanotechnol., 7, 3, 2022, 252-266.
45. D.V. Sridevi, K.T. RamyaDevi, N. Jayakumar, E. Sundaravadivel, pH dependent synthesis of TiO_2 nanoparticles exerts its effect on bacterial growth inhibition and osteoblasts proliferation, AIP Adv., 10, 9, 2020, 095119.
46. Y.O. Fitriyani, U. Septiani, D. . Wellia, R.A. Putri, Safni, Degradation of direct red-23 dye by photolysis with the addition of C-N-codoped TiO_2 catalyst, J. Kim. Valensi, 3, 2, 2017, 152-159.
47. S. Jamil, R. Afzal, S.R. Khan, M. Shabbir, N. Alhokbany, S. Li, R.S.A. Janjua, Photocatalytic degradation of indigo carmine dye by hydrothermally synthesized graphene nanodots (GNDs): investigation of kinetics and thermodynamics, RSC Adv., 2024, 23973-23986.
48. D.J. Ahmed, B.I. Al-Abdaly, S.J. Hussein, synthesis and characterization of high surface area nano titanium dioxide, J. Pet. Res. Stud., 11, 4, 2021, 51-75.
49. K.M. Reza, A.S.W. Kurny, F. Gulsha, Parameters affecting the photocatalytic degradation of dyes using TiO_2: a review, Appl. Water Sci., 7, 2017, 1569-1578.
50. H.D. Tran, D.Q. Nguyen, P.T. Do, U.N.P. Tran, Kinetics of photocatalytic degradation of organic compounds: a mini- review and new approach, RSC Adv., 13, 2023, 16915-16925.
51. H.A. Kiwaan, T.M. Atwee, E.A. Azab, A.A. El-Bindary, Photocatalytic degradation of organic dyes in the presence of nanostructured titanium dioxide, J. Mol. Struct., 1200, 2020, 127115.
52. A. Kumar, G. Pandey, A review on the factors affecting the photocatalytic degradation of hazardous materials, Maters. Sci. Eng. Int. J., 1, 3, 2017, 106-114.
53. F.A. Aisien, N.A. Amenaghawon, E.F. Ekpenisi, Photocatalytic decolourisation of industrial wastewater from a soft drink company, J. Eng. Appl. Sci., 9, 2013, 11-16.
54. H. Ayoub, M. Kassir, M. Raad, H. Bazzi, A. Hijazi, Effect of dye structure on the photodegradation kinetic using TiO_2 nanoparticles, J. Mater. Sci. Chem. Eng., 5, 2017, 31-45.
55. C.M. Antonio-Cisneros, M.M. Davila- Jimenez, M.P. Elizalde-Gonzalez, E. Garcia-Diaz, TiO_2 immoblized on Manihot carbon: Optimal preparation and evaluation of its activity in the decomposition of indigo carmine, Int. J. Mol. Sci., 16, 2015, 1590-1612.
56. V. Gilja, Z. Katancic, L. Kratofil krehula, V. Mandic, Z. Hrnjak-Murgic, Efficiency of TiO_2 catalyst supported by modified waste fly ash ash during photodegradation of RR45 dye, Sci. Eng. Compos. Mater., 26, 2019, 292-300.
57. V.V. Kovalevskiy, A.V. Emeline, V.N. Kuznetsov, N. Serpone, Photoactivity of nanocrystalline TiO_2 under visible light: effect of surface fluorination, J. Phys. Chem. C, 114, 2010, 13494-13500.